CELL BIOLOGY

The Batten disease gene product CLN5 is the lysosomal bis(monoacylglycero)phosphate synthase

Uche N. Medoh[1,2,3,4], Andy Hims[1,2,3]†, Julie Y. Chen[1,2,3]†, Ali Ghoochani[1,2,3], Kwamina Nyame[1,2,3,4], Wentao Dong[1,2,3], Monther Abu-Remaileh[1,2,3]*

Lysosomes critically rely on bis(monoacylglycero)phosphate (BMP) to stimulate lipid catabolism, cholesterol homeostasis, and lysosomal function. Alterations in BMP levels in monogenic and complex neurodegeneration suggest an essential function in human health. However, the site and mechanism responsible for BMP synthesis have been subject to debate for decades. Here, we report that the Batten disease gene product CLN5 is the elusive BMP synthase (BMPS). BMPS-deficient cells exhibited a massive accumulation of the BMP synthesis precursor lysophosphatidylglycerol (LPG), depletion of BMP species, and dysfunctional lipid metabolism. Mechanistically, we found that BMPS mediated synthesis through an energy-independent base exchange reaction between two LPG molecules with increased activity on BMP-laden vesicles. Our study elucidates BMP biosynthesis and reveals an anabolic function of late endosomes/lysosomes.

Bis(monoacylglycero)phosphate (BMP), also known as lysobisphosphatidic acid, is conserved from bacteria to most eukaryotes (*1*, *2*). BMP is an anionic, late endosome/lysosome (LE/LY)-specific glycerophospholipid with unusual esterification, unsaturation, and stereochemistry. BMP potently activates lipid catabolism on intraluminal vesicles (ILVs), promotes lysosomal cholesterol egress, and regulates the formation of ILVs in LE/LYs to maintain cellular homeostasis (*3*–*5*). Notably, lysosomal dysfunction is a hallmark of neurodegeneration, and myriad studies report aberrant abundances of BMP in rare and common neurodegenerative diseases. Of these, neuronopathic lysosomal storage disorders (LSDs), Alzheimer's disease, Parkinson's disease, and frontotemporal dementia are among the most studied (*6*–*10*). Beyond neurodegeneration, BMP function is also implicated in atherosclerosis, drug-induced phospholipidosis, viral infection, and cancer (*11*–*17*). Given its stimulatory effect on lysosomal function, it is speculated that BMP accumulation in certain diseases is an ameliorative, firefighter response to lysosomal dysfunction (*18*–*20*), suggesting that inducing its synthesis may have a major therapeutic benefit in a wide spectrum of human diseases. However, the molecular mechanism responsible for BMP synthesis has been poorly understood for decades, mystifying the role of BMP in disease (*21*).

CLN5 loss substantially reduces BMP

We have been studying the function of genes whose biallelic loss of function results in a family of neurodegenerative LSDs collectively called neuronal ceroid lipofuscinosis (NCL) or Batten disease (*22*, *23*). NCLs are characterized by the accumulation of lipofuscin, infantile to juvenile onset neurodegeneration, and premature death (*24*). We were particularly interested in the soluble *CLN5* gene product given its earlier disease onset, association with Alzheimer's disease, and lack of known molecular function (*22*). Because several reports associate Batten disease with defective lipid metabolism (*9*, *25*), we used untargeted lipidomics to analyze the lipidome of *CLN5* knockout HEK293T lysosomes (fig. S1A) (*26*). We found a massive accumulation of lysophosphatidylglycerol (LPG), a detergent-like lysophospholipid (Fig. 1A and table S1). The acyl composition of LPG did not affect the accumulation phenotype, suggesting that the entire LPG class is uniformly aberrant (Fig. 1A). Notably, we also observed a marked depletion of a glycerophospholipid species consistent with BMP (Fig. 1A). BMP species were uniformly depleted in *CLN5* knockout HEK293Ts (Fig. 1B). The levels of other abundant lipid phosphatidylcholine (PC) were unchanged, and thus were used for normalization hereafter (fig. S1B). Given the alterations in LPG and BMP, we sought to quantitate their levels in *CLN5* knockout HEK293Ts at the whole-cell and lysosomal level using optimized, sensitive multiple reaction monitoring transitions for each class. This targeted analysis confirmed LPG accumulation and BMP deficiency (Fig. 1, B and C, and fig. S1B). Consistent with the exclusive localization of BMP to LE/LYs (*27*), whole cells were comparably deficient in BMP and exhibited similar LPG storage (Fig. 1, B and C, and fig. S1B).

To test whether *CLN5* loss of function affects BMP homeostasis in physiologically relevant systems, we generated CLN5-deficient human induced pluripotent stem cells (iPSCs) and differentiated them into neurons (iNeurons) (fig. S1C). Consistent with results in *CLN5* knockout HEK293Ts, targeted quantitation of BMP and LPG in CLN5-deficient iPSCs and iNeurons revealed substantial storage of LPG and depletion of BMP species at the whole-cell level (Fig. 1D). Thus, CLN5 loss of function depletes BMP levels.

CLN5 is the BMP synthase

The depletion of lysosomal BMP in *CLN5* knockout cells suggests a defect in BMP synthesis. However, despite the well-substantiated role of phosphatidylglycerol (PG) in BMP synthesis (*28*, *29*), CLN5-deficient lysosomes did not accumulate PG (fig. S1D) (*28*, *29*), but showed a minor decrease in few lysosomal PG species, which might be explained by increased catabolism and/or defective lysosomal trafficking. Conversely, LPG, which has been suggested to serve as a direct precursor for BMP, accumulated substantially (Fig. 1, A, C, and D) (*29*, *30*). Consistent with its potential role in BMP synthesis, biochemical fractionation studies support the existence of a lysosomal transacylase that mediates the formation of BMP from LPG and instead indicate that PG deacylation to LPG may be a distinct, upstream biochemical step (*31*, *32*). We were thus intrigued by the presence of two apposed, hydrophobic grooves in an experimental CLN5 crystal structure and a report of hydrolase activity against a monoacylated, anionic tool compound with LPG isosterism (fig. S2, A and B) (*33*). This led us to test whether CLN5 is the elusive BMP synthase.

We expressed and purified recombinant, His-tagged CLN5 to homogeneity as a multimeric protein (fig. S3, A to D), which possessed weak thioesterase activity (fig. S3E). Taking care to carry out experiments below the critical micellar concentration of LPG (18:1) (*34*), we then incubated recombinant CLN5 protein with LPG (18:1) at acidic pH and allowed the reaction to proceed for 15 minutes. Quantitation of LPG (18:1), BMP (18:1/18:1), and its predicted byproduct glycerophosphoglycerol (GPG) revealed the presence of BMP (18:1/18:1) and GPG only in conditions containing CLN5 and LPG (Fig. 2, A, B, and C). We validated the glycerophospholipid as BMP (18:1/18:1) against a synthetic standard (Fig. 2D); thus, we hereafter refer to CLN5 as lysosomal BMP synthase (BMPS).

A kinetic enzyme assay of BMPS activity against LPG, monitoring for BMP and GPG release, yielded moderate enzyme activity (K_{cat}/K_m = ~10^4 M^{-1} s^{-1}) for both products (Fig. 2E and fig. S4A). As a result, the kinetic quantitation of GPG product was used for all further BMPS assays. Notably, removal of the polyhistidine tag did not alter BMPS activity (fig. S4B). Consistent with its LE/LY localization, BMPS synthesized BMP at a slightly acidic optimum of 6.5 with a catalytic efficiency of

[1]Department of Chemical Engineering, Stanford University, Stanford, CA 94305, USA. [2]Department of Genetics, Stanford University, Stanford, CA 94305, USA. [3]The Institute for Chemistry, Engineering & Medicine for Human Health (Sarafan ChEM-H), Stanford University, Stanford, CA 94305, USA. [4]Department of Biochemistry, Stanford University School of Medicine, Stanford, CA 94305, USA.
*Corresponding author. Email: monther@stanford.edu
†These authors contributed equally to this work.

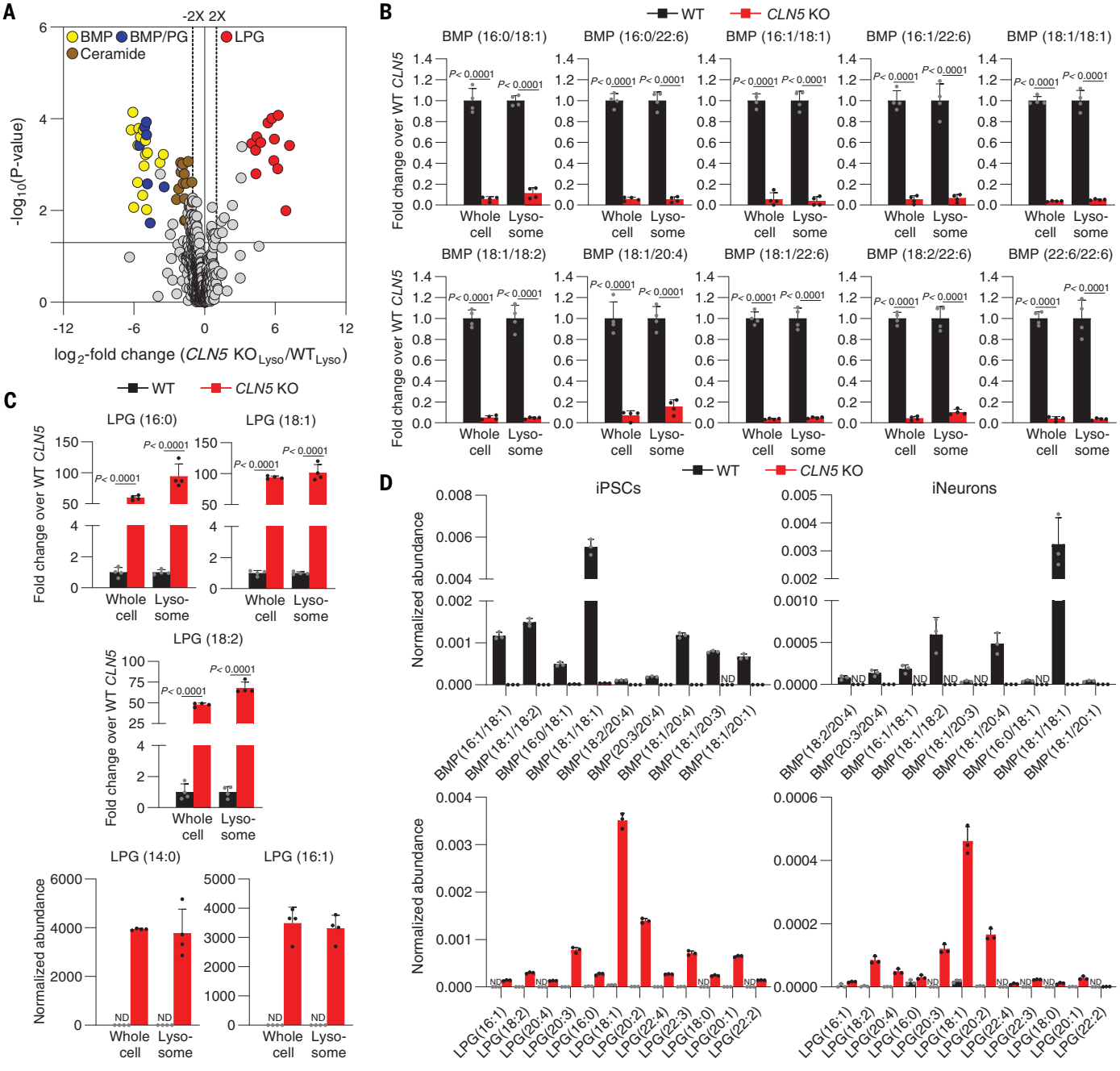

Fig. 1. CLN5 deficiency results in BMP depletion and LPG accumulation. (**A**) Untargeted lipid analysis of HEK293T lysosomes upon *CLN5* loss. Data presented as volcano plot of log_2-transformed fold change in the abundance of lipids between *CLN5* knockout and wild-type HEK293T lysosomes. Significantly altered lipids include LPG (red) and BMP (yellow). BMP/PG (blue) annotation indicates compounds for which fragmentation data was not acquired. Data in table S1. The horizontal line indicates a *P*-value of 0.05 and the vertical line indicates a fold change of 2. Each genotype measurement represents $n = 4$ biologically independent samples. *P*-values were calculated by one-way analysis of variance (ANOVA) with Tukey honestly significant difference (HSD) test and corrected by the Benjamini-Hochberg method with an FDR = 5%. (**B** and **C**) Targeted analyses of BMP and LPG in whole cells and lysosomes. Fold changes in lysosomal BMPs and LPGs between *CLN5* knockout and wild-type HEK293T cells were calculated after subtracting background from control samples and normalizing to endogenous lipid. If species is not detected in wild-type cells, normalized abundance is presented. Data presented as mean ± SD of $n = 4$ biologically independent samples. (**D**) Targeted lipid analysis of LPG and BMP normalized abundances from CLN5-deficient iPSCs and iNeurons compared with the WT. Plotted values are normalized to endogenous lipids. Data presented as mean of $n = 3$ biologically independent samples. ND, not detected. WT, wild-type.

$\sim 10^5\ M^{-1}\ s^{-1}$ although appreciable activity is still retained at a more acidic pH (fig. S4, C and D). To rule out exclusive activity for LPG (18:1), we tested BMPS activity with LPG species of varying lengths. BMPS displays activity against all tested LPGs (LPG 14:0, LPG 16:0, LPG 18:0, LPG 18:1) with a higher preference for longer chain lengths (fig. S4E).

BMPS N143S is a patient missense mutation known to retain protein folding and lysosome trafficking (*35*). Consistent with this literature, we did not observe alterations in recombinant BMPS N143S secondary structure, conformation, and thermal stability relative to the wild type (WT) (fig. S3F, fig. S5A, and fig. S6A). Still,

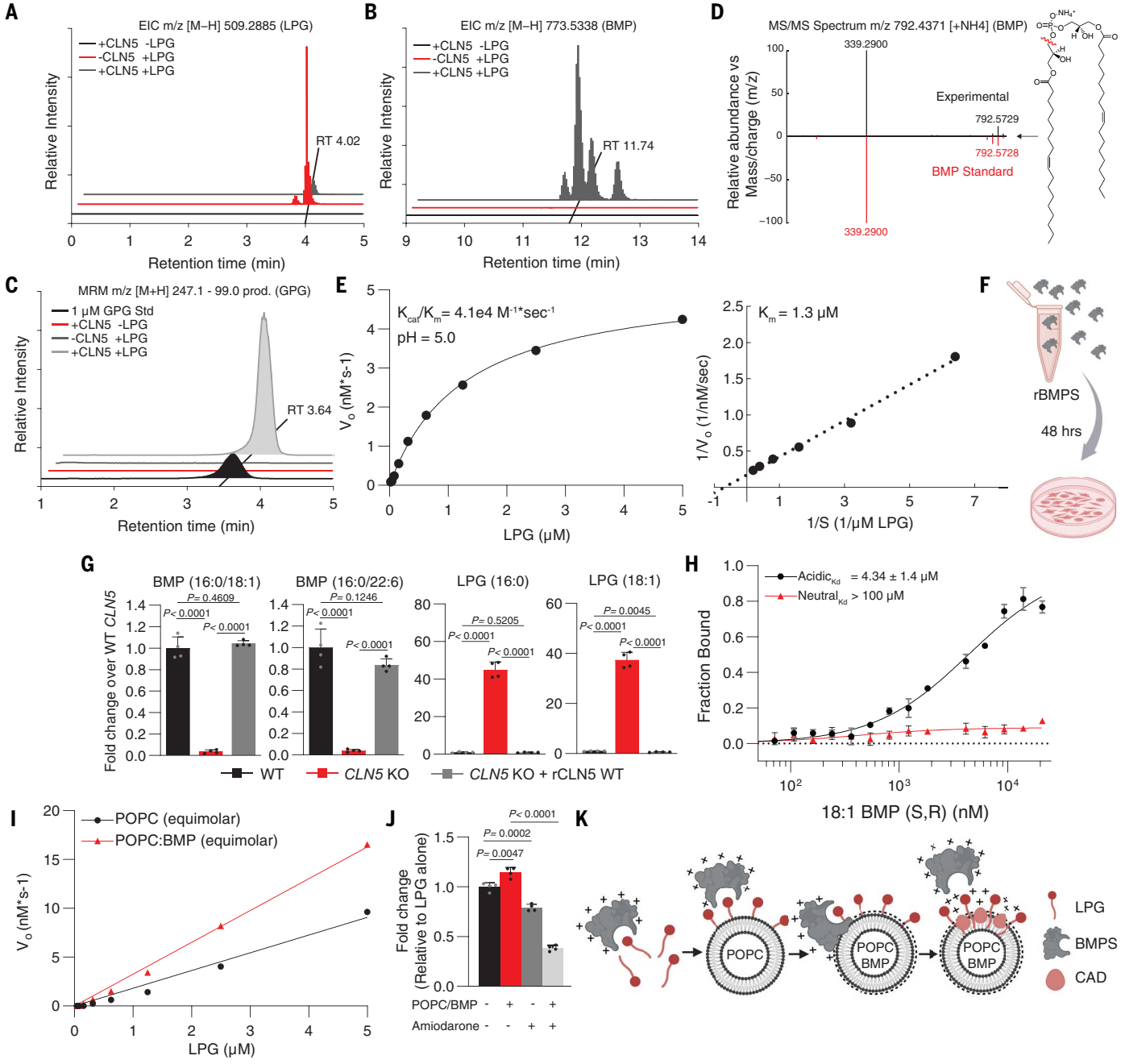

Fig. 2. *CLN5* is the bis(monoacylglycero)phosphate synthase (BMPS). (**A** and **B**) Recombinant CLN5 synthesizes BMP. Representative extracted ion chromatograms (EIC) for LPG (18:1) and BMP (18:1/18:1) from a reaction between recombinant CLN5 and LPG (18:1) under acidic conditions (pH = 5). Retention time corresponds to 3,3′ BMP isoform though acyl migration may occur in vitro. (**C**) BMPS activity results in glycerophosphoglycerol (GPG) release. Representative EIC for GPG byproduct release. (**D**) MS/MS spectral confirmation of CLN5-synthesized BMP (18:1/18:1) compared with commercial standard. (**E**) BMPS is a moderately active enzyme. (Left) Representative Michaelis-Menten curve (MM) for BMPS activity toward LPG (18:1) using GPG to monitor the reaction in acidic conditions. (Right) Lineweaver-Burk transformation of MM curve. Experiment was performed at least three times. K_{cat} (catalytic rate constant) and K_m (Michaelis constant) (**F**) Schematic for recombinant BMPS (rBMPS) supplementation experiment. HEK293T-conditioned media were supplemented with rBMPS for 48 hours prior to lipid analysis. (**G**) rBMPS rescues BMP deficiency and LPG storage. Fold changes in levels of BMP and LPG species were normalized to endogenous lipid. Data presented as mean ± SD of $n = 4$ biologically independent samples. (**H**) BMPS interacts with BMP liposomes. Recombinant BMPS was incubated with 75:25% mol POPC:BMP (18:1/18:1) liposomes under acidic and neutral conditions until reaction reached equilibrium tested by repeated temporal measurements. Data presented as mean ± SD of $n = 3$ technical replicates. Experiment was performed at least three times (**I**) BMP-laden liposomes stimulate BMP synthesis. Recombinant BMPS was incubated with either 100% mol POPC or 75:25% mol POPC/BMP (18:1/18:1) liposomes containing equimolar LPG (18:1). Representative graph shown for experiment performed at least three times. (**J**) Amiodarone inhibits BMPS activity toward monomeric and liposomal LPG. Recombinant BMPS was incubated with either monomeric LPG (18:1) or liposomal LPG (18:1) in the presence or absence of amiodarone. Data presented as mean ± SD of $n = 4$ biologically independent samples. (**K**) Diagram for BMPS activity at a lipid:water interface. BMP-laden vesicles enhance BMPS activity toward LPG. This activation is significantly inhibited by cationic amphiphilic drugs (CADs) such as amiodarone.

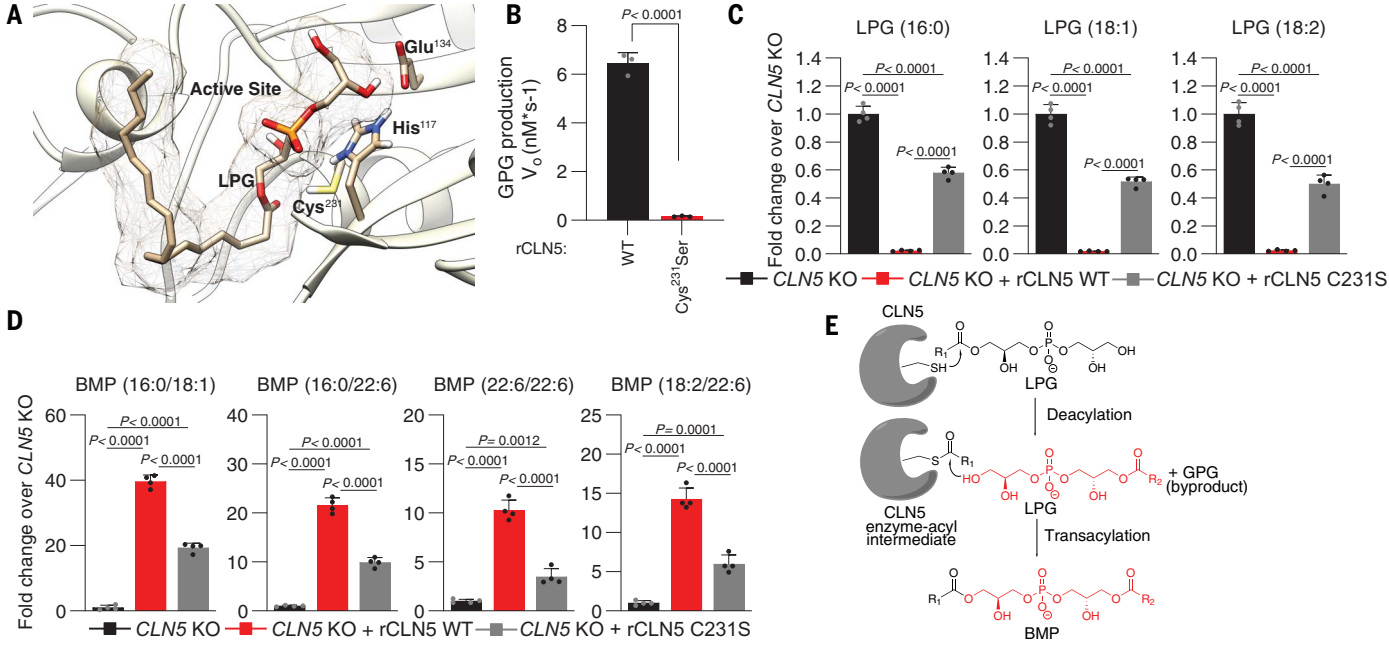

Fig. 3. An active site thiol mediates base exchange for BMP synthesis. (**A**) Schrodinger docking of LPG (18:1) onto an experimental BMPS structure (PDB 6R99). Predicted catalytic triad residues C231, H117, and E134 are annotated. (**B**) Weaker serine nucleophile attenuates BMPS activity as measured by monitoring GPG release. Recombinant BMPS WT and C231S were incubated with LPG (18:1) under acidic conditions. Data presented as mean ± SD of $n = 3$ biologically independent samples. (**C** and **D**) Recombinant BMPS C231S exhibits reduced rescue of LPG storage and BMP deficiency. Fold change in the levels of BMP and LPG species normalized to endogenous lipid. Data presented as mean ± SD of $n = 4$ biologically independent samples. (**E**) Diagram of the BMPS reaction mechanism. The BMPS active site thiol substitutes at the LPG carbonyl carbon releasing a GPG byproduct and abstracting an acyl chain to form a high-energy enzyme-acyl intermediate. Through a base-exchange reaction, the electrophilic intermediate is substituted at its carbonyl carbon by an LPG alcohol to complete the catalytic cycle and release BMP.

BMPS N143S possessed considerably weakened enzyme activity (fig. S7A), suggesting that defective BMP synthesis may drive CLN5 Batten disease.

Several studies support a role of BMPS in endosomal sorting of proteins through extralysosomal secretory compartments such as the endoplasmic reticulum (ER) and Golgi (*22*, *36*, *37*), so we sought to establish a system to evaluate the LE/LY role of BMPS activity in modulating BMP and LPG in live cells. To circumvent the secretory system, we supplemented conditioned media with fluorescently labeled BMPS for endocytic delivery to CLN5 knockout cells and confirmed its localization to LE/LYs by fluorescence microscopy (fig. S8, A to F). With this tool, we tested whether recombinant BMPS replacement in *CLN5* knockout cells can normalize their aberrant lipid profile (Fig. 2F). Recombinant BMPS protein replacement in *CLN5* knockout cells for only 48 hours rescued LPG accumulation and considerably restored BMP levels (Fig. 2G, and fig. S9, A and B). Supplementation of CLN5-deficient cells with recombinant BMPS N143S protein failed to restore LPG and BMP homeostasis (fig. S7, B and C, and fig. S8, B to G). Thus, BMPS localization to the ER or Golgi is not necessary for BMPS activity in cells and the *CLN5* gene product is the lysosomal BMP synthase.

BMP-laden vesicles enhance BMP synthesis

The activation of lipid enzymatic activity through the electrostatic attraction of cationic lysosomal enzymes onto negatively charged ILVs is a central dogma in lysosomal lipid catabolism (*3*, *38*). BMP imbues ILVs with a net negative charge. We thus asked whether BMPS can directly interact with BMP and assessed its functional consequences for BMP synthesis. Indeed, BMPS could only interact with liposomes containing both phosphatidylcholine and BMP and required an acidic pH for docking (Fig. 2H and fig. S10A).

Polyhistidine tags can mediate binding to BMP liposomes (*10*). To rule out a polyhistidine tag–mediated interaction between BMPS and BMP liposomes, we sought to identify the BMPS motif responsible for docking. Previous reports identified an evolutionarily conserved cationic amphipathic helix (CAH) postulated to mediate BMPS anchoring to the lysosome limiting membrane; however, subsequent studies demonstrated that BMPS does not display typical membrane protein characteristics and can be found in soluble fractions following membrane fractionation (*22*). Thus, we asked whether the BMPS CAH instead mediates docking onto ILVs through its well-conserved cationic residues (fig. S10, B and C). Consistent with our hypothesis, mutation of those residues to negatively charged glutamates weakened vesicular BMP binding (fig. S3, G and H, and figs. S5B, S6B, and S10D).

To test for the stimulation of BMPS activity by BMP liposomes, we integrated LPG (18:1) into liposomes at a constant lysophospholipid to liposome equimolar ratio to maintain stimulation of activity and avoid surface dilution (fig. S11A). BMP liposomes enhanced BMP synthesis as expected (Fig. 2I) (*31*). In agreement with the lipid enzyme theory, we observed a surface dilution effect with higher liposome to substrate ratios (fig. S11B) (*39*). Consistent with studies on the ability of other anionic phospholipids to stimulate lysosomal lipid enzymes (*5*, *40*, *41*), we observed increased BMPS activity on membranes containing PG, phosphatidylinositol, and phosphatidylserine, although the relatively high abundance of BMP in ILVs suggests BMP acts as the main anionic coactivator in lysosomes (fig. S11C) (*42*).

Given the stimulation of BMPS activity by BMP liposomes, we asked whether cationic amphiphilic drugs (CAD) inhibit BMP synthesis in the presence and absence of LPG-integrated BMP liposomes. Amiodarone, a CAD shown to cause drug-induced phospholipidosis (*38*), slightly inhibited BMPS activity toward nonliposomal LPG and dramatically inhibited BMPS activity toward liposomal LPG likely through

neutralization of the negative charge on the surface of BMP liposomes (Fig. 2, J and K) (*38*). Altogether, these data support a role of BMP in stimulating LE/LY lipid anabolism.

A base-exchange reaction mediates BMP synthesis

A base-exchange reaction between two LPG molecules mediates BMP synthesis in fractionated lysosomal lysates (*30*). Such a reaction mechanism should result in an initial release of glycerophosphoglycerol during LPG deacylation without any energy input. Supporting this mechanism, we detected the water-soluble GPG byproduct along with BMP (Fig. 2C). In principle, the base-exchange reaction could utilize any lysophospholipid as an acyl donor, so we asked whether other lysophospholipids—namely lysophosphatidylcholine (LPC)—lysophosphatidylserine (LPS), lysophosphatidylethanolamine (LPE), and lysophosphatidylinositol (LPI), are additional BMPS substrates. With an equimolar amount of lysophospholipid and LPG, we did not detect an appreciable release of glycerophosphocholine, glycerophosphoserine, glycerophosphoethanolamine, nor glycerophosphoinositol to support their involvement in BMP synthesis (fig. S12A). Consistent with these in vitro findings, LPC, LPE, and LPS did not accumulate in BMPS-deficient lysosomes, and LPI only modestly increased (fig. S12, B to E, and table S1). Thus, LPG represents an exclusive lysophospholipid acyl donor for base exchange.

In silico docking experiments identified a plausible active site that positioned the LPG carbonyl carbon near a cysteine 231, histidine 117, and glutamate 134 catalytic triad (Fig. 3A) (*33*). Given the predicted cysteine nucleophile, the BMPS thioester enzyme-acyl intermediate mimics an acyl-CoA coenzyme utilized by acyltransferases for extralysosomal lipid synthesis (*43*). Because thiols are more nucleophilic than alcohols, and the thioester enzyme-acyl intermediate represents a stronger electrophile than its ester counterpart for base exchange with an LPG alcohol, we asked whether a cysteine-to-serine BMPS substitution attenuates enzyme activity (figs. S3I, S5C, and S6C). Consistent with this idea, the weaker C231S BMPS retained less than 5% of the wild-type BMPS activity when monitoring GPG release (Fig. 3B and fig. S12F), and its replacement in *CLN5* knockout cells for 48 hours only partially rescued LPG accumulation and BMP deficiency relative to that of wild-type BMPS (Fig. 3, C and D, fig. S8, B to F and H, and fig. S12, G and H). These data support an energy-independent, active site thiol-mediated base exchange for BMP synthesis (Fig. 3E).

Late endosomes/lysosomes require BMPS to synthesize BMP

Given the localization of BMPS to lysosomes and the lysosomal deficiency of BMP, we sought to confirm whether LE/LYs, known for their degradative capacity, are the site of BMP synthesis (*32*). To this end, we leveraged an established method to conjugate lipid tracers to bovine serum albumin (BSA) for efficient endocytic internalization and delivery (Fig. 4A) (*44*). To *CLN5* knockout cells we fed a BSA-conjugated, deuterium-labeled (d5-)PG (16:0/18:1) tracer at various time points and assessed conversion of PG to LPG and BMP in LE/LYs by monitoring the appearance of deuterium-labeled metabolites (Fig. 4B). *CLN5* knockout cells converted d5-PG (16:0/18:1) to d5-LPG (18:1) with comparable kinetics to the WT but exhibited a complete block in d5-LPG (18:1) conversion to d5-BMP (18:1/18:1) (Fig. 4C and fig. S13A). Notably, *CLN5* knockout cells showed no decrease in uptake of the d5-PG (16:0/18:1) precursor whose levels were higher in knockout cells compared with the WT, suggesting higher endocytic uptake (fig. S13B). Thus, LE/LYs of *CLN5* knockout cells are unable to transform LPG into BMP, consistent with the molecular function of BMPS to mediate transacylation of LPG to form BMP. To further confirm LE/LYs as the site of BMP synthesis, we used the LysoIP system to monitor BMP synthesis in vitro (*26*). To this end, we immunoprecipitated BMPS-deficient LE/LYs and assessed their ability to convert deuterated PG to BMP (Fig. 4D). Indeed, BMPS-deficient lysosomal lysates were unable to convert d5-PG (16:0/18:1) to d5-BMP (18:1/18:1) and d5-BMP (16:0/18:1) (Fig. 4E). Complementation of BMPS-deficient lysosomal lysate with recombinant CLN5 restored synthesis of d5-BMP (18:1/18:1) and d5-BMP (16:0/18:1) (Fig. 4E).

Consistent with the ability of BMP to stimulate phospholipase activity (*38*), *CLN5* knockout cells fed with a BSA-conjugated d9-PC (18:0/18:0) tracer at various timepoints displayed reduced kinetic conversion of d9-PC (18:0/18:0) to d9-LPC (18:0), suggesting weakened phospholipase activity (Fig. 4, F and G). Endocytic uptake of d9-PC (18:0/18:0) was comparable between wild-type and *CLN5* knockout cells, with a slight increase in knockout cells if any (fig. S13C).

BMP is also known to stimulate glycosphingolipid catabolism within late endosomes/lysosomes (*9*). We thus tested whether CLN5 loss of function affects glucosylceramidase (GCase) activity. Indeed, CLN5-deficient HEK293Ts exhibited slower conversion of d5-Glc1Cer (d18:1/18:0) to d5-Cer (d18:1/18:0) without reduced endocytic uptake, indicating attenuated GCase activity (Fig. 4, H and I, and fig. S13D). CLN5 knockout HEK293T cells, iPSCs, and iNeurons did not exhibit an increase in the levels of hexosylceramides (fig. S14A) although CLN5 knockout HEK293T cells and iPSCs were deficient in ceramides, which were largely unaffected in iNeurons (fig. S14B). Still, CLN5 knockout iNeurons accumulated GM3 gangliosides (Fig. 4J), another lipid whose degradation is dependent on BMP. Notably, such gangliosidosis is known to drive neurodegeneration (*10*).

Given the role of BMP in stimulating ILV biogenesis (*4*), we asked whether CLN5-deficient HEK293Ts exhibit alterations to ILV abundance. Consistent with this idea, the number of ILVs in CLN5-deficient lysosomes was substantially reduced (Fig. 4K). BMP is necessary for LE/LY cholesterol homeostasis (*45*, *46*). Consistent with this idea, filipin staining revealed accessible cholesterol storage in *CLN5* knockout cells (Fig. 4L). Treatment of *CLN5* knockout cells with recombinant BMPS significantly rescued secondary cholesterol storage material below WT levels consistent with BMP's role in maintaining intracellular cholesterol homeostasis (Fig. 4L). Thus, CLN5 is the elusive BMPS whose function is essential for proper lipid catabolism and trafficking in the lysosome.

Discussion

Despite the discovery of BMP over a half a century ago, the machinery responsible for its synthesis has remained enigmatic. We identify the Batten disease gene product CLN5—whose loss leads to neurodegeneration—as the elusive BMPS (*47*). BMPS utilizes two lysophosphatidylglycerol molecules in an energy-independent fashion to synthesize BMP, the activation of which occurs on BMP-enriched ILVs. This base-exchange reaction represents the first example of anabolism within a harsh, digestive lysosomal environment and provides a reaction mechanism for other potential anabolic processes within this classically catabolic organelle.

Several questions regarding the BMP biosynthetic pathway remain. First, lysosomes are thought to contain a small amount of PG if any at all. It is thus unclear what subcellular compartment supplies the initial PG substrate for BMP synthesis. Given the nearly exclusive localization of PG in mitochondria where it serves as a precursor for cardiolipin, it is attractive to theorize that mitochondria-lysosome crosstalk is required for BMP synthesis (*48*). Second, a lysosomal phospholipase that mediates the conversion of PG to LPG in LE/LYs was recently identified (*49*), and whether other phospholipases play a role in BMP synthesis through substrate production is unknown (*32*). Furthermore, BMP exhibits an unusual (S,S) stereochemistry that may be produced by an isomeric transformation of LPG (*50*). Whether this transformation occurs spontaneously or through the action of an unidentified LPG isomerase remains to be determined. Lastly, how biallelic mutations in BMPS result in CNS-restricted pathology is unclear. Although it is possible that BMP metabolism is most relevant in the CNS where post mitotic, long-lived neurons heavily rely on lysosomes to maintain neuronal homeostasis (*51*), we speculate that other enzymes/proteins may compensate for BMPS loss of function. Indeed, BMPS acts in a complex with

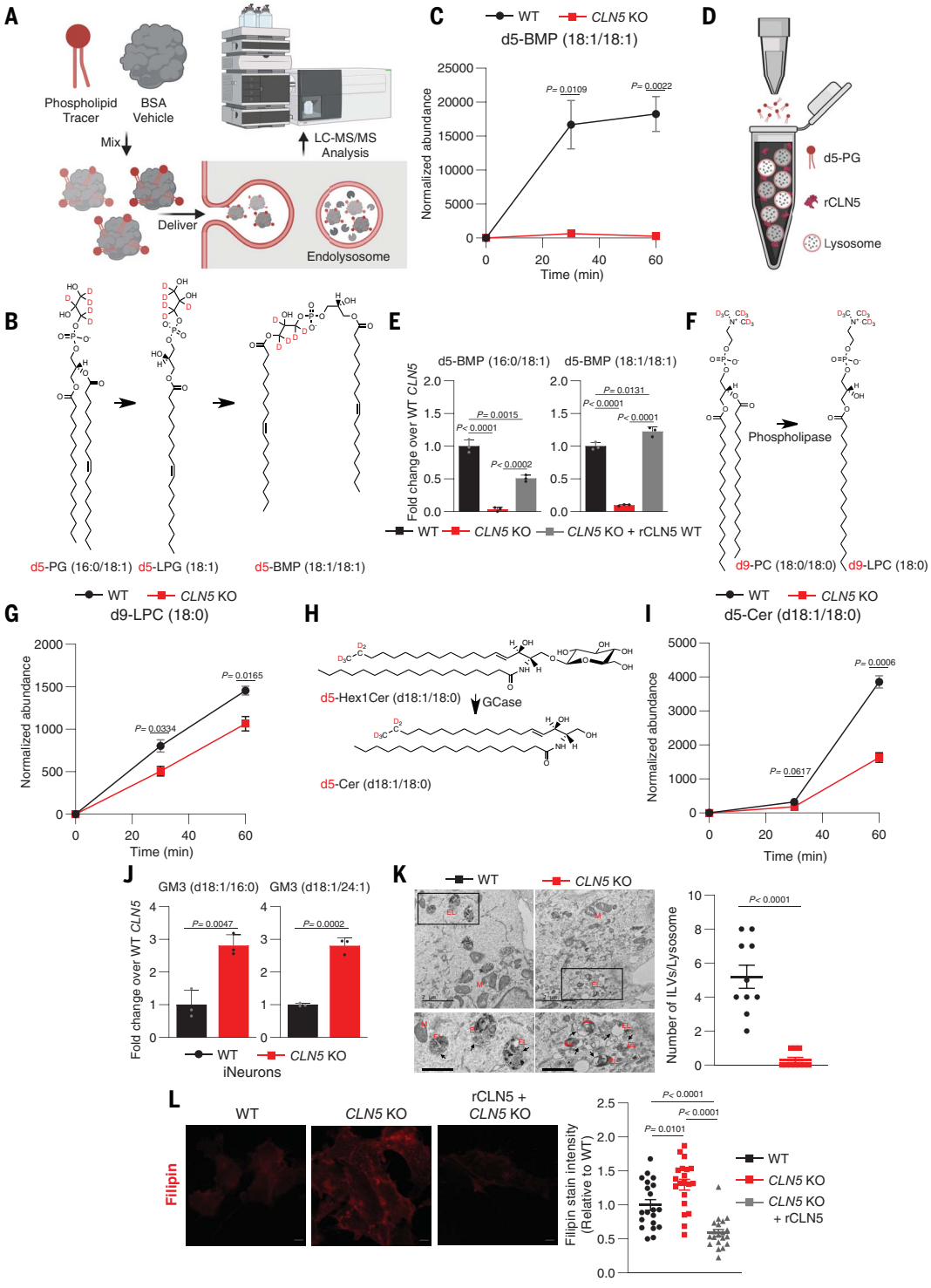

Fig. 4. Late endosomes/lysosomes synthesize BMP to maintain lipid homeostasis. (**A**) Schematic for LE/LY delivery of deuterated tracers for metabolism and LC-MS/MS analysis. Deuterated lipids are conjugated to BSA and supplemented in HEK293T-conditioned media after starvation to increase endocytic flux. After several time points, lipids were extracted for LC-MS/MS analysis. (**B**) Depiction of monitored deuterated phosphatidylglycerol metabolites bearing 5 deuterium atoms in their glycerol moiety. (**C**) *CLN5* knockout HEK293Ts are unable to synthesize deuterated BMP. Intensities for d5-BMP (18:1/18:1) in *CLN5* knockout and wild-type HEK293T cells are presented after background subtraction and normalization to endogenous lipids. Data presented as mean ± SD of $n = 3$ biologically independent samples. (**D**) Schematic for recombinant BMPS complementation experiment in BMPS deficient lysosomal protein extract. Lysosomes were immunoprecipitated and harvested for proteins. Lysosomal proteins were complemented with recombinant BMPS and supplied with d5-PG (16:0/18:1) under acidic conditions. (**E**) Lysosomal lysates require BMPS to synthesize BMP. Fold change in the levels of synthesized deuterated BMP species. Data presented as mean ± SD of $n = 3$ biologically independent samples. (**F**) Depiction of monitored deuterated phosphatidylcholine metabolites bearing 9 deuterium atoms in their methyl groups. (**G**) *CLN5* knockout HEK293T lysosomes exhibit impaired phospholipid catabolism. Intensities for d9-LPC (18:0) production in *CLN5* knockout and wild-type HEK293T cells are presented after background subtraction and normalization to endogenous lipids. Experiment was done as in (A). Data presented as mean ± SD of $n = 3$ biologically independent samples. (**H**) Depiction of monitored deuterated glucosylceramide metabolites bearing 5 deuterium atoms in their hydrocarbon chain (**I**) *CLN5* knockout HEK293T lysosomes exhibit impaired GCase activity. Intensities for d5-Hex1Cer (d18:1/18:0) production in *CLN5* knockout and wild-type HEK293T cells are presented after background subtraction and normalization to endogenous lipids. Experiment was done as in (A). Data presented as mean ± SD of $n = 3$ biologically independent samples. (**J**) CLN5-deficient iNeurons accumulate GM3 gangliosides. Fold changes in lipid species abundance between *CLN5* knockout and wild-type HEK293T cells were calculated after subtracting background from control samples and normalizing to endogenous lipids. Data presented as mean ± SD of $n = 3$ biologically independent samples. (**K**) BMPS-deficient HEK293Ts have fewer ILVs. Representative electron micrographs of *CLN5* knockout and wild-type HEK293T cells. The average number of ILVs within each identified endolysosome per cell are counted with 10 cells per condition. Arrows indicate ILVs. Scale bars, 2 μm. Inset scale bar, 1 μm. EL, endo-lysosome; M, mitochondria. (**L**) BMPS deficient HEK293T cells accumulate cholesterol. Filipin staining of cholesterol in recombinant BMPS-treated and -untreated *CLN5* knockout and wild-type HEK293T cells was determined and are presented relative to WT. Representative data shown for experiment repeated at least three times with 20 cells per condition. Scale bar = 10 μm.

CLN3 to regulate retromer function, and it is unknown whether this function is directly linked to BMP synthesis (*36*, *37*).

Several studies reveal a deficiency of BMP in other mutated Batten disease genes (CLN3, CLN11) or alterations in BMPS lysosomal trafficking and/or abundance by loss of other Batten disease gene products (CLN6, CLN7, CLN8, CLN14) (*9*, *10*, *25*, *47*, *52*–*54*). Given the identification of the Batten disease *CLN5* gene product as the BMPS, BMP dyshomeostasis may be the unified metabolic defect in Batten disease. Future studies should investigate the potential biochemical role of Batten disease gene products in maintaining BMP homeostasis.

BMP is implicated in a wide spectrum of diseases and processes, such as atherosclerosis, drug-induced phospholipidosis, viral infection, cancer, and neurodegeneration (*6*–*17*). Given the critical function of lysosomes in these contexts, we hypothesize that BMP may play a fundamental, protective role in maintaining cellular homeostasis and may promote processes that influence virulence and cancer. The identification of BMPS provides an opportunity to study the role of BMP in lysosomal biology and disease using genetic and chemical tools and positions BMPS as an attractive therapeutic target.

REFERENCES AND NOTES

1. D. R. Body, G. M. Gray, *Chem. Phys. Lipids* **1**, 254–263 (1967).
2. S. Czolkoss *et al*., *Environ. Microbiol.* **23**, 6993–7008 (2021).
3. H. D. Gallala, K. Sandhoff, *Neurochem. Res.* **36**, 1594–1600 (2011).
4. H. Matsuo *et al*., *Science* **303**, 531–534 (2004).
5. A. Abe, J. A. Shayman, *J. Lipid Res.* **50**, 2027–2035 (2009).
6. U. N. Medoh, J. Y. Chen, M. Abu-Remaileh, *Curr. Opin. Syst. Biol.* **29**, 100408 (2022).
7. A. M. Miranda *et al*., *Transl. Psychiatry* **12**, 129 (2022).
8. R. N. Alcalay *et al*., *Mov. Disord.* **35**, 134–141 (2020).
9. T. Logan *et al*., *Cell* **184**, 4651–4668.e25 (2021).
10. S. Boland *et al*., *Nat. Commun.* **13**, 5924 (2022).
11. M. Arnal-Levron, Y. Chen, I. Delton-Vandenbroucke, C. Luquain-Costaz, *Biochem. Pharmacol.* **86**, 115–121 (2013).
12. N. Liu, E. A. Tengstrand, L. Chourb, F. Y. Hsieh, *Toxicol. Appl. Pharmacol.* **279**, 467–476 (2014).
13. A. Patel, B.-P. Mohl, P. Roy, *J. Biol. Chem.* **291**, 12408–12419 (2016).
14. C. Bissig *et al*., *Dev. Cell* **25**, 364–373 (2013).
15. A. Erazo-Oliveras *et al*., *Cell Chem. Biol.* **23**, 598–607 (2016).
16. T. Kirkegaard *et al*., *Nature* **463**, 549–553 (2010).
17. A. Serrano-Puebla, P. Boya, *Biochem. Soc. Trans.* **46**, 207–215 (2018).
18. O. Ilnytska *et al*., *J. Biol. Chem.* **297**, 100813 (2021).
19. D. Moreau *et al*., *EMBO Rep.* **20**, e47055 (2019).
20. P. A. Lewis, *Sci. Transl. Med.* **14**, eabq7374 (2022).
21. M. R. Showalter *et al*., *Int. J. Mol. Sci.* **21**, 8067 (2020).
22. I. Basak *et al*., *Cell. Mol. Life Sci.* **78**, 4735–4763 (2021).
23. F. M. Platt, A. d'Azzo, B. L. Davidson, E. F. Neufeld, C. J. Tifft, *Nat. Rev. Dis. Primers* **4**, 27 (2018).
24. S. E. Mole, S. L. Cotman, *Biochim. Biophys. Acta* **1852**, 2237–2241 (2015).
25. N. N. Laqtom *et al*., *Nature* **609**, 1005–1011 (2022).
26. M. Abu-Remaileh *et al*., *Science* **358**, 807–813 (2017).
27. T. Kobayashi *et al*., *Nature* **392**, 193–197 (1998).
28. F. Hullin-Matsuda *et al*., *J. Lipid Res.* **48**, 1997–2008 (2007).
29. B. J. Poorthuis, K. Y. Hostetler, *J. Biol. Chem.* **251**, 4596–4602 (1976).
30. J. Heravi, M. Waite, *Biochim Biophys Acta Mol Cell Biol Lipids.* **1437**, 277–286 (1999).
31. S. J. Huterer, J. R. Wherrett, *Biochim Biophys Acta Mol Cell Biol Lipids.* **1001**, 68–75 (1989).
32. B. Amidon, A. Brown, M. Waite, *Biochemistry* **35**, 13995–14002 (1996).
33. A. V. Luebben *et al*., *Sci. Adv.* **8**, eabj8633 (2022).
34. R. E. Stafford, T. Fanni, E. A. Dennis, *Biochemistry* **28**, 5113–5120 (1989).
35. A. Moharir, S. H. Peck, T. Budden, S. Y. Lee, *PLOS ONE* **8**, e74299 (2013).
36. S. Yasa, E. Sauvageau, G. Modica, S. Lefrancois, *Biochem. J.* **478**, 2339–2357 (2021).
37. A. Mamo, F. Jules, K. Dumaresq-Doiron, S. Costantino, S. Lefrancois, *Mol. Cell. Biol.* **32**, 1855–1866 (2013).
38. J. A. Shayman, A. Abe, *Biochim. Biophys. Acta* **1831**, 602–611 (2013).
39. G. M. Carman, R. A. Deems, E. A. Dennis, *J. Biol. Chem.* **270**, 18711–18714 (1995).
40. G. Wilkening, T. Linke, K. Sandhoff, *J. Biol. Chem.* **273**, 30271–30278 (1998).
41. T. Linke *et al*., *Biol. Chem.* **382**, 283–290 (2001).
42. T. Kobayashi *et al*., *J. Biol. Chem.* **277**, 32157–32164 (2002).
43. T. J. Grevengoed, E. L. Klett, R. A. Coleman, *Annu. Rev. Nutr.* **34**, 1–30 (2014).
44. S. G. Scharenberg *et al*., *Sci. Adv.* **9**, eadf8966 (2023).
45. J. Chevallier *et al*., *J. Biol. Chem.* **283**, 27871–27880 (2008).
46. L. A. McCauliff *et al*., *eLife* **8**, e50832 (2019).
47. M. Savukoski *et al*., *Nat. Genet.* **19**, 286–288 (1998).
48. J. A. Mayr, *J. Inherit. Metab. Dis.* **38**, 137–144 (2015).
49. J. Chen *et al*., *Commun. Biol.* **6**, 210 (2023).
50. T. Thornburg, C. Miller, T. Thuren, L. King, M. Waite, *J. Biol. Chem.* **266**, 6834–6840 (1991).
51. V. Udayar, Y. Chen, E. Sidransky, R. Jagasia, *Trends Neurosci.* **45**, 184–199 (2022).
52. Y. Wang *et al*., *Sci. Adv.* **8**, eabm5578 (2022).
53. T. Danyukova *et al*., *Hum. Mol. Genet.* **27**, 1711–1722 (2018).
54. L. Bajaj *et al*., *J. Clin. Invest.* **130**, 4118–4132 (2020).
55. U. N. Medoh, Lipidomic analysis of WT and CLN5-deficient HEK293T cells, iPSCs, and iNeurons. Dryad (2023); https://datadryad.org/stash/dataset/doi:10.5061/dryad.gb5mkkwvq.

ACKNOWLEDGMENTS

We thank all members of the Abu-Remaileh laboratory for valuable discussions. We also thank S. Pfeffer for help and access to MST and nanoDSF instruments, L. Gan for providing the NGN2-iPSCs, and P. Kim for providing Expi293s for protein expression. Additionally, we thank the Metabolomics Knowledge Center (MKC) at Sarafan ChEM-H and the Stanford Neuroscience Microscopy Service at Wu Tsai Neurosciences Institute. **Funding:** This work was supported by the National Institute on Aging of the National Institutes of Health under award P30AG066515 supporting the Stanford Alzheimer's Disease Research Foundation (ADRC) and from Beat Batten and the NCL Foundations (NCL-Stiftung) to M.A-R. This work was further supported by the Knight Initiative for Brain Resilience and the Innovative Medicines Accelerator to M.A-R. U.N.M. and K.N. are supported by the Sarafan ChEM-H Chemistry/Biology Interface Program as O'Leary-Thiry Fellows and Kolluri Fellows, respectively. J.Y.C. was supported by the Chemical Engineering Research Experience for Undergraduates Program. A.H. is supported by the Sarafan ChEM-H/IMA Postbaccalaureate Program in Target Discovery. K.N. is additionally supported by the Bio-X Stanford Interdisciplinary Graduate Fellowship affiliated with the Wu Tsai Neurosciences Institute (Bio-X SIGF: Mark and Mary Steven's Interdisciplinary Graduate Fellow). M.A-R. is a Stanford Terman Fellow and a Pew-Stewart Scholar for Cancer Research, supported by The Pew Charitable Trusts and the Alexander and Margaret Stewart Trust. **Author contributions:** U.N.M. and M.A-R. conceptualized the study. U.N.M. designed and performed experiments with assistance from J.Y.C. and A.H. A.G. genetically modified and maintained iPSCs. U.N.M. and K.N. developed targeted mass spectrometry methods. U.N.M., K.N., and W.D. acquired mass spectrometry data. U.N.M. and W.D. analyzed mass spectrometry data. U.N.M. and M.A-R. wrote the manuscript, and all other authors reviewed its contents. **Competing interests:** U.N.M. and M.A-R. are inventors on a patent related to this work filed by Stanford University. M.A-R. is a scientific advisory board member of Lycia Therapeutics. All other authors declare no competing interests. **Data and materials availability:** All data is available in the main text or the supplementary materials. Plasmids and cell lines can be requested from, and requests will be fulfilled by, the corresponding author. Lastly, we have provided the raw data in a public repository for the lipidomic analyses in Fig. 1 (A and D) (*55*).

SUPPLEMENTARY MATERIALS

science.org/doi/10.1126/science.adg9288
Materials and Methods
Figs. S1 to S14
Table S1
References (*56*, *57*)
MDAR Reproducibility Checklist

Submitted 31 January 2023; resubmitted 4 May 2023
Accepted 16 August 2023
10.1126/science.adg9288